MARTIAN DUST SIZE AND SHAPE FROM NAVCAM AND HAZCAM IMAGES ON MSL

H. Chen-Chen[1], S. Pérez-Hoyos[1], and A. Sánchez-Lavega[1]
[1]Dep. Física Aplicada I, ETS Ingenieros Bilbao, University of the Basque Country (UPV/EHU), Bilbao, Spain.

Introduction: Although not designed for this specific purpose, images obtained by the Mars Science Laboratory (MSL) engineering cameras can be used for retrieving the atmospheric optical depth and dust aerosol physical properties at Gale Crater [12], [14]. The objective of this study is to validate the use of the MSL engineering cameras for retrieving the amount of dust aerosol suspended in the Martian atmosphere, characterize its physical properties and study its temporal and seasonal variation through the MSL mission.

MSL Engineering Cameras: The MSL Curiosity rover is equipped with 12 cameras with the objective of supporting the surface operations of the rover by providing views of the surrounding terrain and characterising the position and orientation of the rover and its robotic arm [9] (see Figure 1). These engineering cameras are build-to-print copies of the Mars Exploration Rover (MER) cameras [8], the Navigation Cameras (*Navcam*) consist of four cameras mounted on the remote sensing mast with a 45-degree square field of view an a broadband response span of 600-850 nm; while the Hazard Avoidance Cameras (*Hazcam*) are chassis-mounted tactical fish-eyed cameras located at the front and rear of the vehicle with a 124-degree square FOV.
Complete technical specifications for the MSL engineering cameras can be found in [8], [9].

Observation data: The dust size distribution and particle shape can be constrained by evaluating the sky brightness as a function of the angle from the Sun [14], [17]. Navcam has accumulated more than 7,000 sky pointing images covering almost 3 Martian Years; while Hazcam have obtained more than 17,000 wide angle images in a regular basis using its front and rear cameras.
In order to characterise the dust particle forward scattering properties, we have evaluated 200 Navcam and Hazcam Sun pointing images spanning for 120 different mission sols through MSL mission. In addition to this, dust phase function backward scattering region was evaluated using Navcam sky surveys and Hazcam wide-field backward-pointing images and reaching high scattering angles up to 160º for constraining the dust particle shape.

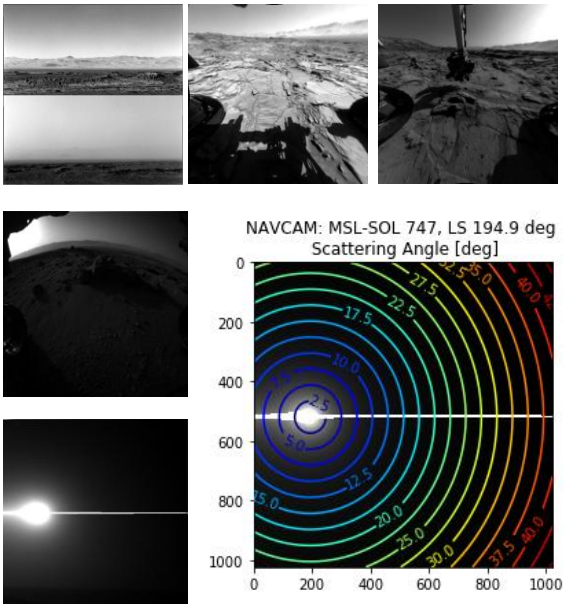

Figure 1: *(Top-row) Examples of MSL engineering cameras retrieved images. (Bottom-left) Sun-pointing observations from Hazcam (top) and Navcam (bottom) used in this study. (Bottom-right) An example is provided for Navcam MSL sol 747 showing the derived scattering angle contour lines for the scene after the image calibration and photogrammetic reduction.*

MSL engineering camera images were calibrated using the pipepline developed by Soderblom et al. [13], and the photogrammetric reduction was done using the JPL camera pointing CAHVOR model [2], [4] (see Figure 1).

Methodology: We use radiative transfer modelling of the sky brightness observed by the MSL cameras to constrain the atmospheric dust loading (optical depth), the dust aerosol size distribution and the particle shape. For each image, the observed sky britghtness as a function of the scattering angle is compared to a model data computed for specific values of these variables, using a Chi-square best fitting criteria.

The engineering cameras upward-looking observations are modelled using a 30-layers plane-parallel multiple scattering radiative transfer code DISORT [16] implemented in Python (PyDISORT) [1]; the atmosphere model vertical profiles for the structure (e.g., pressure, temperature, density, composition) are retrieved from the Mars Climate Database GCM [3], [10], for the time, period and location (Mars' Gale Crater) of the observation, gas species absorption and opacity are calculated from the parameters on Hitran 2012 database [13]. Dust aerosol particles are modelled using a T-Matrix code [11] for different shapes, dust optical properties are retrieved from Wolff et al., [19] and a modified gamma particle size distribution [5] is employed for a 0.35 fixed effective variance [7].

Results: In Figure 2 we display the optical depth at MSL location along 1650 sols (spanning MY 31-33) and the retrieved relation ship between particle effective radius and optical depth.

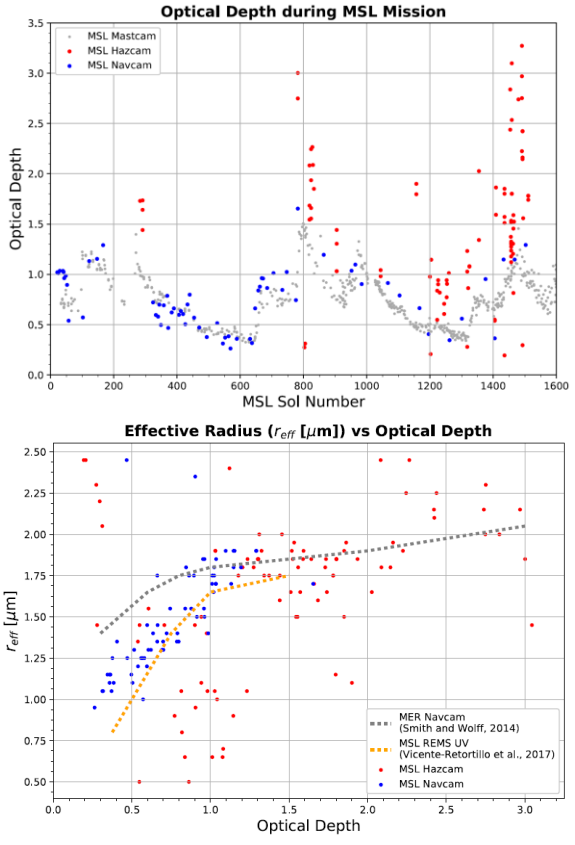

Figure 2: (Top) Navcam (blue) and Hazcam (red) retrieved optical depths compared to Mastcam (gray) 880nm Sun direct imaging tau values [6]. (Bottom) Particle size distribution effective radius values (in microns) for almost 3 Martian Years mission.

Conclusions: We show in this study that radiative transfer results validate the use of MSL engineering camera observations for retrieving the dust optical depth and constraining the aerosol particle shape and size distribution. The retrieved column optical depth values agrees with MSL Mastcam Sun direct imaging measurements [6]. Seasonal differences are observed for the effective radius (radii between 1.0 and 1.3 microns during low dust season, steep increase to peak values up to 1.90 microns during dust season Ls 150-300 deg; presenting similar trends when comparing with other authors [14], [15], [18] (see Figure 2)

References:

[1] Adamkovics, M. et al., **Icarus** 270, 376-388, 2016.
[2] Di, K., and Li, R., **JGR** 109, E04004, 2004.
[3] Forget, F., et al., **JGR** 104, 24155-24176, 1999.
[4] Gennery, D. B., **Int. J. Comput.** 68(3), 239-266, 2006.
[5] Hansen, J. E., and Travis, L. D., **Space. Sci. Rev.** 16, 527-610, 1974.
[6] Lemmon, M. T., **8th Int. Conf. on Mars**, Abstract #1338, 2014.
[7] Madeleine, J.-B., et al., **JGR** 116, E11010, 2011.
[8] Maki, J. N., et al., **JGR** 108, 8071, 2003.
[9] Maki, J. N., et al., **Space Sci.Rev.** 170, 77-93, 2012.
[10] Millour, E., et al., **EPSC Abstracts** vol. 10, EPSC2015-438, 2015.
[11] Mishchenko, M. I., et al., **J. Quan. Spec. Rad. Trans.** 88, 357-406, 2004.
[12] Moore, C. A., et al., **Icarus** 264, 102-108, 2016.
[13] Rothman, L. S., et al., **J. Quan. Spec. Rad. Trans**. 130, 4-50, 2013
[14] Smith, M. D., and Wolff, M. J., **5th MAMO**, Abstract #2101, 2014.
[15] Soderblom, J. M., et al., **JGR** 113, E06S19, 2008.
[16] Stamnes, K. et al., **App.Opt**. 27, 2502-2509, 1998.
[17] Tomasko, M. G., **JGR** 104, 8987-9007, 1999.
[18] Vicente-Retortillo, A., et al., **GRL** 44, 3502-3508, 2017.
[19] Wolff, M. J., et al., **JGR** 114, E00D04, 2009.

Acknowledgements: This work was supported by the Spannish project AYA2015-65041-P with FEDER support, Grupos Gobierno Vasco IT-765-13, and Diputación Foral de Bizkaia - Aula EspaZio Gela.